

**Rapid Communications**

---

*The Rapid Communications section is intended for the accelerated publication of important new results. Manuscripts submitted to this section are given priority in handling in the editorial office and in production. A Rapid Communication may be no longer than 3½ printed pages and must be accompanied by an abstract. Page proofs are sent to authors, but, because of the rapid publication schedule, publication is not delayed for receipt of corrections unless requested by the author.*

---

**High-resolution electron-energy-loss-spectroscopy study of the oxidation of Al(111)**

J. L. Erskine and R. L. Strong

*Department of Physics, The University of Texas, Austin, Texas 78712*

(Received 16 February 1982)

High-resolution electron-energy-loss spectra are reported which describe the oxidation of Al(111) surfaces. The initial stage of oxidation is characterized by both surface and subsurface atomic oxygen. The surface oxygen phase is unstable and converts to subsurface oxygen at room temperature. No evidence of molecular oxygen adsorption is observed. The dipole scattering mechanism is found to apply to "subsurface" dipoles near metal surfaces.

The oxidation of Al(111) surfaces has been the subject of several recent experimental<sup>1-6</sup> and theoretical investigations.<sup>7-9</sup> Two independent studies which combine photoemission and surface extended x-ray absorption fine structure (EXAFS) reach different conclusions regarding the initial stage of Al(111) surface oxidation and the associated atomic level structure. Bachrach *et al.*<sup>1</sup> suggest that room-temperature oxidation of Al(111) proceeds in three phases: a molecular phase produced by doses below 100 L ( $1 \cdot L = 1 \times 10^{-6}$  Torr sec) at  $2 \times 10^{-7}$  Torr, a surface atomic phase produced after doses greater than 150 L, at  $2 \times 10^{-7}$  Torr, and a subsurface oxygen phase produced by doses greater than 125 L at  $1 \times 10^{-6}$  Torr. Norman *et al.*<sup>2</sup> report two phases of oxygen on Al(111) corresponding to surface and subsurface oxygen. The subsurface phase is reported to occur upon heating to 200 °C, and both phases are reported to form simultaneously for oxygen exposures greater than 50 L.

Low-energy-electron diffraction (LEED) studies place surface oxygen at a distance  $Z = 1.46$ ,<sup>3</sup>  $1.33^4$  and  $1.54 \text{ \AA}$  (Ref. 5) above the surface plane in the threefold hollow site. Other LEED studies<sup>6</sup> report a  $(1 \times 1)$  oxygen underlayer with  $Z = 0.73 \text{ \AA}$  and an overlayer with  $Z = 0.8 \text{ \AA}$ . Recent theoretical studies<sup>7,8</sup> yield values between  $Z = 0.55$  and  $0.62 \text{ \AA}$  for surface oxygen at the threefold hollow site, and have also suggested an underlayer<sup>9</sup> could account for many of the reported experimental results. The surface EXAFS studies also provide values for  $Z$ : Bachrach *et al.*<sup>1</sup> predict for surface oxygen  $Z = 0.98 \text{ \AA}$  and Norman *et al.*<sup>2</sup> predict for both surface and underlayer oxygen  $Z = 0.60 \text{ \AA}$ . Work-function measurements<sup>10-13</sup> give inconsistent results, but most experi-

ments observe a small decrease in work function ( $\Delta\phi < 200 \text{ meV}$ ) for light oxygen doses (50 L or less) suggesting that surface chemisorption dominates low coverage behavior.

In this Communication, we report studies of the oxidation of Al(111) using high-resolution electron-energy-loss spectroscopy (EELS). Our results show that room-temperature oxidation of Al(111) involves both surface and subsurface oxygen even at very low doses. In addition, our results show that the surface oxygen phase is unstable and converts at room temperature to subsurface oxygen. These new results help account for many of the discrepancies in experimental work on the Al(111) oxygen system and provide a more informed basis for attempting to arrive at accurate structural models using surface EXAFS and LEED.

Experiments reported here were conducted using a spectrometer which incorporates tandem EELS optics, 4-grid LEED optics, and twin-pass cylindrical mirror analyzer Auger optics. X-ray Laue techniques and spark erosion were used to align and cut 1-mm-thick Al targets having a (111) crystal axis parallel ( $\pm 1^\circ$ ) to the surface normal. Rods from which the crystals were cut were obtained from Metron Inc. and were 99.999+ % pure. *In situ* cleaning was accomplished by repeated cycles of argon ion sputtering (500 eV,  $10 \mu\text{A}$ ) and annealing at 500 K. Clean targets yielded excellent LEED patterns and exhibited only minute traces of C, O, and Ar in Auger spectra. Base pressures were maintained in the  $10^{-11}$ -Torr range.

Figure 1 illustrates EELS spectra for Al(111) exposed at 300 K to 2, 20, and 200 L of oxygen at  $2 \times 10^{-7}$  Torr. Two peaks dominate the loss spectra. The lower-energy peak (80 meV) is attributed to a

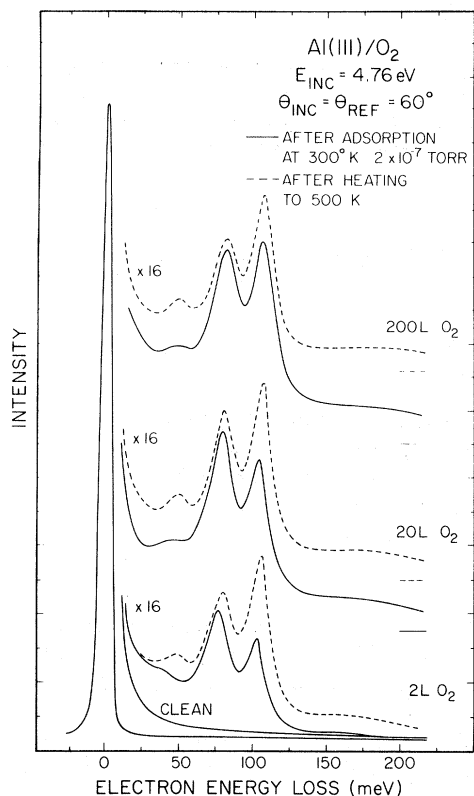


FIG. 1. EELS spectra for Al(111) exposed at 300 K to 2, 20, and 200 L of oxygen at  $2 \times 10^{-7}$  Torr (solid curves) corresponding spectra after heating to 500 K (dashed curves). Scattering angles,  $\theta$ , are measured from the surface normal. Electron impact energy  $E_{inc} = 4.76$  eV. Baselines for each curve are indicated to the right. All spectra were normalized so that elastic peak intensities were equal and scale factors indicated are relative to the elastic peak.

stretch mode perpendicular to the surface involving oxygen at the threefold hollow surface site. The higher-energy peak (105 meV) is attributed to a stretch mode perpendicular to the surface involving oxygen at the threefold hollow site below the surface. These assignments are discussed in more detail later. From the data shown in Fig. 1 and similar spectra at other pressures we have shown that *both* surface and subsurface sites are occupied when room-temperature Al(111) is exposed to oxygen. Low doses ( $< 50$  L) favor the surface sites, but even 1-L doses produce mixed phases containing a fairly large fraction of subsurface oxygen. Later we argue that the two peak intensities correspond approximately to the relative surface and subsurface concentrations. Heating always increases the subsurface-to-surface oxygen ratio, and higher doses yield, at any temperature, a higher concentration of subsurface oxygen.

The initial phase of oxygen chemisorption on Al(111) is unstable at room temperature. Figure 2 il-

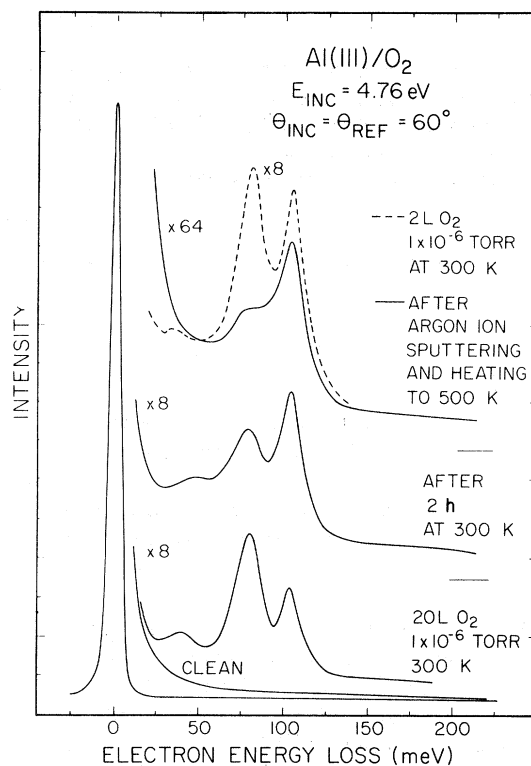


FIG. 2. Lower two curves: EELS spectrum taken immediately after exposing a 300 K Al(111) surface to 20 L of oxygen and a second spectrum taken one hour later. Relative peak heights illustrate the instability of the surface oxygen phase. Upper EELS spectra show that mild sputtering decreases the surface oxygen peak in relation to the subsurface peak.

lustrates the instability. The lower spectrum was obtained immediately after exposing a clean room-temperature Al(111) surface to a 20-L dose at  $1 \times 10^{-6}$  Torr; the middle spectrum was taken two hours later. The vacuum system pressure, after the 20-L dose, was below  $1 \times 10^{-10}$  Torr. Similar results were obtained for other oxygen doses with the sample maintained at 300 K. We conclude that 300 K is sufficient to activate formation of the subsurface oxygen phase from chemisorbed surface oxygen. This result does not appear unreasonable. Small temperature increases greatly accelerate the formation of subsurface oxygen. We also note that subsurface and surface oxygen vibrational energies are nearly equal, suggesting that both sites have approximately the same formation energy. In addition, we note that instability of the  $(1 \times 1)$  oxygen layer has been suggested by Hofmann *et al.*,<sup>14,15</sup> who have conducted careful work-function and photoemission studies of this system.

Assignment of the two major EELS spectra peaks to surface chemisorbed oxygen ( $E = 80$  meV) and to

subsurface oxygen ( $E = 105$  meV) is unambiguous. The dose and temperature dependence of these peaks correspond to photoemission observations<sup>1,2</sup> of the Al2*p* core level shifts which are attributed to surface and subsurface oxygen phases, and are also consistent with basic results of work-function<sup>14,15</sup> and ellipsometry studies.<sup>16</sup> The spectra shown in the upper portion of Fig. 2 confirm assignment of the higher-energy peak to subsurface oxygen. Starting with a surface having both surface and subsurface oxygen peaks, gentle argon ion sputtering is observed to reduce the peak attributed to surface oxygen in relation to the other peak. This result confirms our peak assignment. EELS spectra taken after exposing Al(111) surfaces at 500 K to 3000-L oxygen doses exhibit features totally different from the spectra for surface and subsurface oxygen. Figure 3 shows an EELS spectrum for oxidized Al(111) presumed to closely approximate crystalline Al<sub>2</sub>O<sub>3</sub>. The primary loss peak at  $E = 110$  meV corresponds to the 940-cm<sup>-1</sup> (118-meV) reflectance minimum observed in infrared reflectance from Al<sub>2</sub>O<sub>3</sub> samples.<sup>17,18</sup> We find no evidence for molecular oxygen adsorption over the temperature range of our present experiments, which is 300–500 K.

It is not unreasonable that EELS is able to probe subsurface oxygen, at least in the present case. Scattering of low-energy electrons by a dipole placed below a metal surface has been discussed by Rahman, Black, and Mills.<sup>19</sup> The potential produced by a subsurface dipole can be estimated using the Thomas-Fermi model to account for screening by conduction electrons. In this model the potential strength is governed by the factor.

$$\phi_{\text{dipole}} \propto 2e^{-k_{\text{TF}}d},$$

where  $k_{\text{TF}}$  characterizes the Thomas-Fermi screening length and  $d$  is the distance the dipole moment is located below the surface. As  $k_{\text{TF}}d \rightarrow 0$  the potential approaches the same result obtained for a dipole placed just above the surface. Theoretical predictions<sup>7</sup> and estimates based on LEED<sup>6</sup> and surface EXAFS<sup>2</sup> indicate  $Z \approx 0.6$  Å for subsurface oxygen; and the effective dipole distance  $d$  will be smaller. Therefore  $k_{\text{TF}}d \leq 1$  should be valid for the Al(111) oxygen underlayer. This result represents our rationale for stating that the underlayer and surface dipoles yield approximately equal scattering cross sections, thus permitting quantitative estimates of the concentrations of each phase based on EELS peak weights. We varied the impact energy between 5 and 17 eV and did not observe any significant changes in the

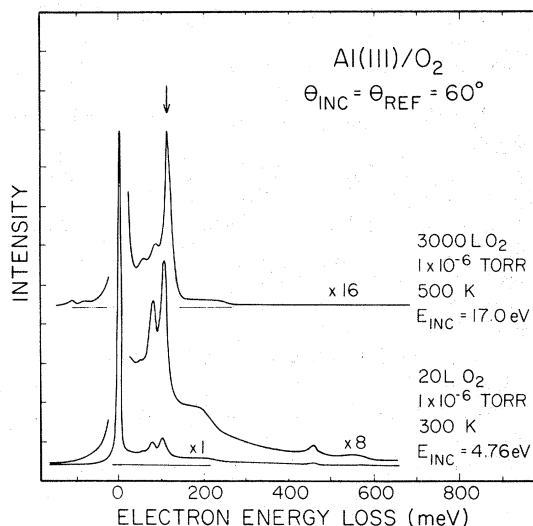


FIG. 3. Lower EELS spectrum corresponds to surface and subsurface oxygen after 12 h. Upper EELS spectrum corresponds to Al<sub>2</sub>O<sub>3</sub>. Arrow shows position of dominant infrared absorption for Al<sub>2</sub>O<sub>3</sub> at 118 meV (940 cm<sup>-1</sup>) (Refs. 17 and 18). The peak at 463 meV corresponds to the O–H stretch of adsorbed OH groups.

peak ratios.

In summary, we have shown that the initial state of oxidation of 300-K Al(111) surfaces involves both surface and subsurface oxygen. Although our results are consistent with general conclusions drawn previously from photoemission, ellipsometry, and work-function studies, our results also show that particular care will be required to extract bond distances from LEED and surface EXAFS results because of the mixed nature of low coverage oxide phases. The instability of the surface phase further complicates the experimental situation. Low-temperature work may be necessary to isolate the surface and subsurface oxygen phases. The relatively rapid conversion of chemisorbed surface oxygen to a mixed phase undoubtedly accounts for many of the experimental discrepancies observed in studies of this system.

#### ACKNOWLEDGMENTS

This work was sponsored by the Air Force Office of Scientific Research under Grant No. AFOSR-80-0154 and by an NSF Equipment Grant No. DMR-81-06049.

- <sup>1</sup>R. Z. Bachrach, G. V. Hansson, and R. S. Bauer, *Surf. Sci.* **109**, L560 (1981).
- <sup>2</sup>D. Norman, S. Brennan, R. Jaeger, and J. Stohr, *Surf. Sci.* **105**, L297 (1981).
- <sup>3</sup>H. L. Yu, M. C. Munoz, and F. Soria, *Surf. Sci.* **94**, L184 (1980).
- <sup>4</sup>C. W. B. Martinson, S. A. Flodström, J. Rundgren, and P. Westrin, *Surf. Sci.* **89**, 102 (1979).
- <sup>5</sup>R. Payling and J. A. Ramsey, *J. Phys. C* **13**, 505 (1980).
- <sup>6</sup>F. Soria, V. Martinez, M. C. Munoz, and J. L. Sacedón, *Phys. Rev. B* **24**, 6926 (1981).
- <sup>7</sup>D. M. Bylander, L. Kleinman, and K. Mednick (unpublished).
- <sup>8</sup>N. D. Lang and A. R. Williams, *Phys. Rev. Lett.* **34**, 531 (1975); *Phys. Rev. B* **18**, 616 (1978).
- <sup>9</sup>L. Kleinman, and K. Mednick, *Phys. Rev. B* **23**, 4960 (1981).
- <sup>10</sup>P. O. Gartland, *Surf. Sci.* **62**, 183 (1979).
- <sup>11</sup>P. Hofmann, W. Wyrobisch, and A. M. Bradshaw, *Surf. Sci.* **80**, 344 (1979).
- <sup>12</sup>W. Eberhardt and F. J. Himpsel, *Phys. Rev. Lett.* **42**, 1375 (1979).
- <sup>13</sup>R. Michel, J. Gastaldi, C. Allasia, and C. Jordan, *Surf. Sci.* **95**, 309 (1980).
- <sup>14</sup>P. Hofmann, W. Wyrobisch, and A. M. Bradshaw, *Surf. Sci.* **80**, 344 (1980).
- <sup>15</sup>P. Hofmann, C. Munschwitz, K. Horn, K. Jacobi, A. M. Bradshaw, and K. Kambe, *Surf. Sci.* **89**, 322 (1979).
- <sup>16</sup>B. E. Hayden, W. Wyrobisch, W. Opperman, S. Hachichia, P. Hofmann, and A. M. Bradshaw, *Surf. Sci.* **109**, 207 (1981).
- <sup>17</sup>E. P. Mertens, *Surf. Sci.* **71**, 161 (1978).
- <sup>18</sup>J. Chantelet, H. H. Classen, D. M. Gruen, I. Sheft, and W. B. Wright, *Appl. Spectrosc.* **29**, 185 (1975).
- <sup>19</sup>T. S. Rahman, J. E. Black, and D. L. Mills, *Phys. Rev. B* **25**, 883 (1982).